Phys Chem Minerals (2008) 35:137–145
DOI 10.1007/s00269-007-0205-3

ORIGINAL PAPER

Photoluminescence spectra of S_2^- center in natural and heat-treated scapolites

Aierken Sidike · I. Kusachi · S. Kobayashi · K. Atobe · N. Yamashita

Received: 17 July 2007 / Accepted: 9 November 2007 / Published online: 14 December 2007

Abstract The emission and excitation spectra of yellow luminescence due to S_2^- in scapolites (#1 from Canada and #2 from an unknown locality) were observed at 300, 80 and 10 K. Emission and excitation bands at 10 K showed vibronic structures with a series of maxima spaced 15–30 and 5–9 nm, respectively. The relative efficiency of yellow luminescence from scapolite #2 was increased up to 117 times by heat treatment at 1,000°C for 2 h in air. The enhancement of yellow luminescence by heat treatment was ascribed to the alteration of SO_3^{2-} and SO_4^{2-} to S_2^- in scapolite.

Keywords Scapolite · Photoluminescence · S_2^- center · Heat treatment

Introduction

The natural scapolite represented by the general formula $(Na,Ca)_4Al_3(Al,Si)_3Si_6O_{24}(Cl,CO_3)$ is the solid solution of marialite (Ma) $Na_4Al_3Si_9O_{24}Cl$ and meionite (Me) $Ca_4Al_6Si_6O_{24}CO_3$. The crystal structures of various types of natural scapolite were investigated by many researchers (Shaw 1960; Chappell and White 1968; Lin and Burley 1975; Curie et al. 1981; Swayze and Clark 1990; Teertstra and Sherriff 1996; Seto et al. 2004). In accordance with the nomenclature of Shaw (1960), the scapolites are classified into marialite, Me_0–Me_{20}; dipyre, Me_{20}–Me_{50}; mizzonite, Me_{50}–Me_{80}; meionite, Me_{80}–Me_{100}. Scapolite shows a strong yellow fluorescence band with a distinct vibronic structure, which is evident even at room temperature. Early reports on the photoluminescence (PL) spectra of natural scapolite were reviewed by Kirk (1955), who treated the luminescence and tenebrescence of natural and synthetic sodalites, and observed the PL spectra of natural scapolite at 293 and 77 K under 365.0 nm excitation. The features of the PL spectra of scapolite were similar to those of natural sodalite and hackmanite, and the PL spectra of scapolite extended from about 500 to 700 nm and consisted of broad bands with structures whose most intense peaks were located at 570 and 589 nm at 293 and 77 K, respectively (Kirk 1955). Kirk (1955) ascribed the orange–yellow fluorescence of sodalite and the yellow fluorescence of scapolite to the presence of sodium polysulfide.

Since 1960, the optical properties of O_2^-, S_2^-, $SeS^-$and Se_2^- ions in various alkali–halide crystals have been investigated by some researchers (Rolfe et al. 1961; Rolfe 1964, 1968; Kirk et al. 1965; Ikezawa and Rofe1973; Rebane and Rebane 1974).

From the analogy of bimolecular ion centers in alkali–halide crystals, the yellow fluorescence of scapolite has been ascribed to S_2^- ions (Tarashchan 1978; Burgner et al. 1978; Marfunin 1979; Curie et al. 1981; Prokofiev et al. 1982; Gorobets and Rogojine 2002). The crystal structure of the scapolite family is formed from open aluminosilicate

Aierken Sidike
School of Mathematics, Physics and Information Sciences, Xinjiang Normal University, Urumqi, Xinjiang 830054, China

I. Kusachi
Department of Earth Sciences, Faculty of Education, Okayama University, Tsushima-naka, Okayama 700-8530, Japan

S. Kobayashi
Department of Applied Science, Faculty of Science, Okayama University of Science, Ridai-cho, Okayama 700-0005, Japan

K. Atobe (✉) · N. Yamashita
Department of Physics, Faculty of Education, Okayama University, Tsushima-naka, Okayama 700-8530, Japan
e-mail: atobe@cc.okayama-u.ac.jp

cages consisting of AlO_4 and SiO_4 tetrahedra. These cages contain Na^+, Ca^{2+}, Cl^- and CO_3^{2-} ions, and the dominant S species in scapolite are SO_3^{2-} and SO_4^{2-} substituting for CO_3^{2-} (Chappell and White 1968; Lin and Burley 1975; Curie et al. 1981; Swayze and Clark 1990; Teertstra and Sherriff 1996). Figure 1 shows the S_2^- center in an aluminosilicate cage of scapolite determined by electron paramagnetic resonance (EPR) experiments (Curie et al. 1981).

Tarashchan (1978) observed the emission bands of the S_2^- center in natural scapolite. The emission band showed a distinct structure with the most intense peak located at about 625 nm. Burgner et al. (1978) reported the vibronic structures observed on the emission and excitation bands of S_2^- centers in natural and heat-treated scapolites at 4.2 K. Details will be described in the following section. Curie et al. (1981) observed S_2^- emission bands with the most intense peaks located at about 600 and 599 nm for scapolite at 80 K under pressures of zero and 5.7 kbar, respectively. Prokofiev et al. (1982) observed the S_2^- emission band with the most intense peak located at about 626 nm for meionite.

The objectives of this investigation are to observe the PL spectra of natural and heat-treated scapolites in detail and show the effect of heat treatment on the efficiency of yellow luminescence due to the S_2^- center in scapolite.

Experimental

In this study, two natural scapolites were used, one (#1) from Canada and the other (#2) from an unknown locality. As described in our previous paper (Aierken et al. 2007), the efficiency of the S_2^- luminescence of heat-treated sodalite was about seven times as high as that of untreated natural sodalite. From the analogy of sodalite, we attempted to heat

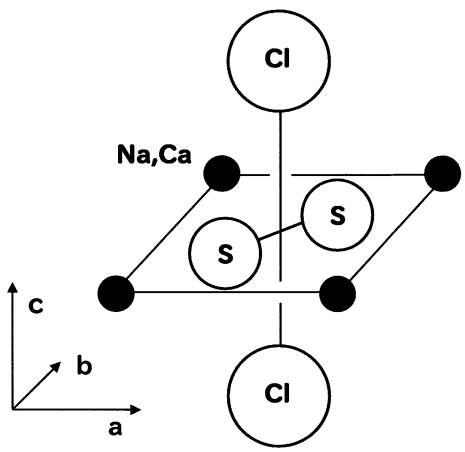

Fig. 1 S_2^- in aluminosilicate cage of scapolite (Curie et al. 1981)

scapolite under various conditions. Before heating, the broken pieces of natural scapolite were powdered using an agate mortar. Scapolites of two forms, powder and broken piece, were heated in quartz crucibles in the temperature range of 600–1,100°C for 15–120 min in air. After heating, the samples were rapidly quenched to room temperature by placing the crucibles on a metal plate. A few samples were kept in a furnace after heating and slowly cooled to room temperature after 4 h.

The crystal structures of the samples were examined using a Rigaku RAD-1B X-ray powder diffraction system. The structures were ascertained by comparing the data with ICDD Cards, 31-1279 for marialite and 2-405 for meionite.

The chemical compositions of the samples were determined using a JEOL JXA-8900 electron probe microanalyser (EPMA) operating at 15 kV and 12 nA with a beam diameter of 5 μm.

In the measurement of the contents of trace elements in the samples, an inductively coupled plasma-optical emission spectrometer (ICP-OES) (Varian, Vista-PRO type) was used. Before ICP-OES analysis, approximately 200 mg of a powdered sample was dissolved in 15 ml nitric acid. The solution was evaporated to dryness. The residue was dissolved in 0.1 M nitric acid to produce 50 ml of the stock solution. The stock solution was examined using the ICP-OES.

Before the measurement of luminescence spectra, the samples were sufficiently powdered using an agate mortar. The powdered samples were packed into sample holders with synthetic quartz–glass covers.

The details of the system for measuring PL and excitation spectra were described in our previous paper (Aierken et al. 2007). In the measurement of luminescence spectra, a 200 W deuterium lamp, a 500 W xenon short-arc lamp and a 50 W halogen tungsten lamp were used as excitation light sources.

In the measurement of PL spectra, excitation wavelengths were selected using a Ritsu MC-50L grating monochromator. A band-pass glass filter or an interference filter was set in front of the sample to eliminate stray light from the excitation source. Observation wavelengths were selected using a Ritsu MC-50 grating monochromator. A suitable glass filter was set in front of the entrance slit of the observation monochromator to eliminate the radiation reflected from the excitation source. The PL spectral intensity was measured using a Hamamatsu Photonics R955 photomultiplier. The PL spectra were corrected for the spectral sensitivity of the measuring system using a standard tungsten lamp calibrated according to the National Bureau of Standards (NBS), USA.

In the measurement of optical excitation spectra, the same measuring system as that used for the emission spectra was used. As excitation light sources, three types of

lamp corresponding to three measurement regions were used: a deuterium lamp in the 190–320 nm region, a xenon short-arc lamp in the 280–400 nm region and a halogen tungsten lamp in the 360–480 nm region. The ordinate of the excitation spectra was plotted against the excitation efficiency after optical excitation energy correction.

Results

The heat-treated scapolite showed intensely bright yellow luminescence under the UV light from a handy Hg lamp (TOPCON FI-5L, 11 W, 365.0 nm). The brightness of yellow luminescence from scapolite #1 heat-treated under optimum conditions exceeded that of yellow luminescence from the well-known phosphor ZnS:Mn under 365.0 nm excitation. The effect of heat treatment did not depend on the sample form, powder or broken piece, or on the speed of thermal quenching after heating.

Figure 2 shows the relative intensities of yellow luminescence from powdered scapolite #2, unheated and heat-treated under various conditions. The PL intensities at room temperature were observed at 596 nm under 390 nm excitation and plotted on a logarithmic scale. Heat treatments for 30 min at 600 and 800°C reduced luminescence efficiencies to about 60% of that unheated powder sample, whereas heat treatments at 1,000°C for 15, 30, 60 and 120 min increased relative luminescence efficiencies to 28, 85, 108 and 117 times, respectively, as high as that of the unheated powder sample.

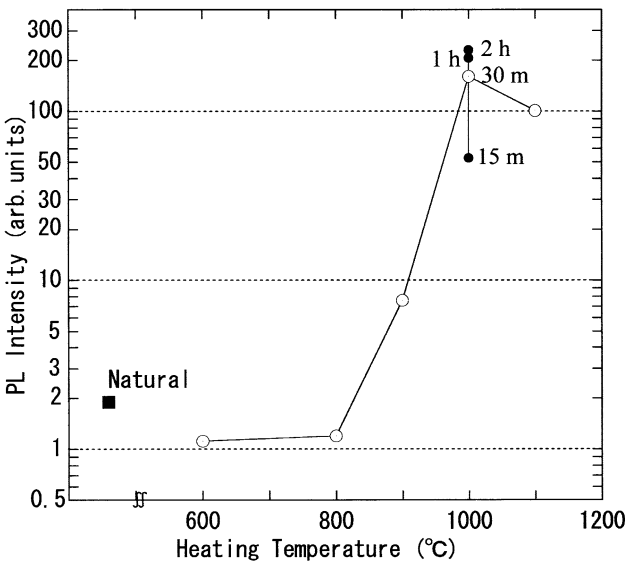

Fig. 2 Relative intensities of yellow luminescence from powdered scapolite #2; unheated (*filled square*), heated for 30 min at various temperatures (*open circle*) and heated at 1,000°C for various times (*filled circle*). The ordinate is plotted on a logarithmic intensity scale

Figure 3 shows the PL spectra of yellow luminescence from four scapolites, natural #1, heat-treated #1 (1,000°C, 30 min), natural #2 and heat-treated #2 (1,000°C, 30 min). The PL intensities were observed at room temperature under 390 nm excitation and plotted on a logarithmic scale. The features of the PL spectra of the four samples were almost the same and the curves were parallel to each other on a logarithmic scale. The relative luminescence efficiency of heat-treated scapolite #1 (Curve 2) was about 11 times as high as that of natural scapolite #1 (Curve 1), whereas that of heat-treated scapolite #2 (Curve 4) was about 85 times as high as that of natural scapolite #2 (Curve 3).

The X-ray patterns of natural scapolite #1 and heat-treated scapolite #1 (1,000°C, 30 min) obtained by a powder diffraction method were almost the same, and the interplanar spacings d (Å) calculated from diffraction lines corresponded well to those for the components of scapolite, namely, marialite and meionaite. Figure 4a, b shows the X-ray patterns of natural scapolite #2 and heat-treated scapolite #2 (1,000°C, 30 min), respectively. Only a minor diffraction line at $2\theta = 29.40°$, which is shown by an arrow in an inset in Fig. 4a, vanished after heating (see inset in Fig. 4b). The line that vanished was assigned to the strongest diffraction line due to calcite. This indicates that the minor inclusion of calcite in natural scapolite #2 was decomposed into noncrystal CaO and CO_2 gas by heating

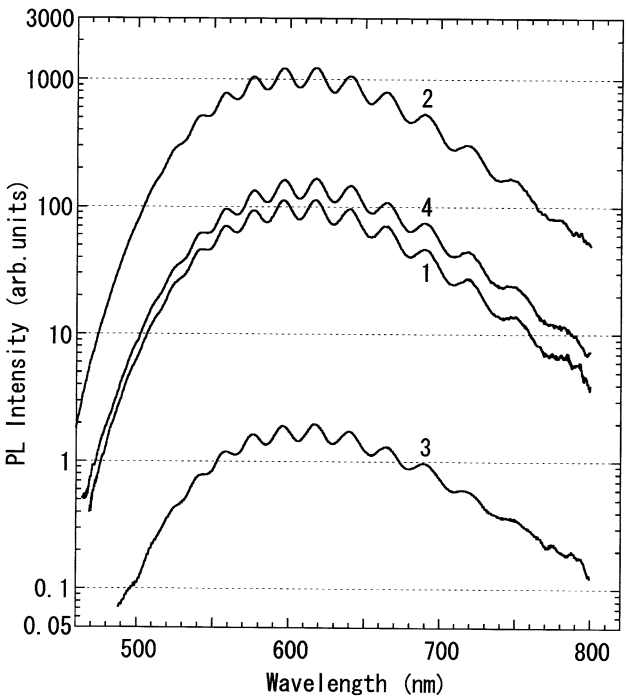

Fig. 3 PL spectra of four scapolites on logarithmic intensity scale, obtained at room temperature under 390 nm excitation; *1* natural scapolite #1, *2* heat-treated scapolite #1 (1,000°C, 30 min), *3* natural scapolite #2 and *4* heat-treated scapolite #2 (1,000°C, 30 min)

in air. Indeed, the mass of powder sacapolite #2 decreased by 1% (600°C, 30 min) to 9% (1,100°C, 30 min) after heat treatment.

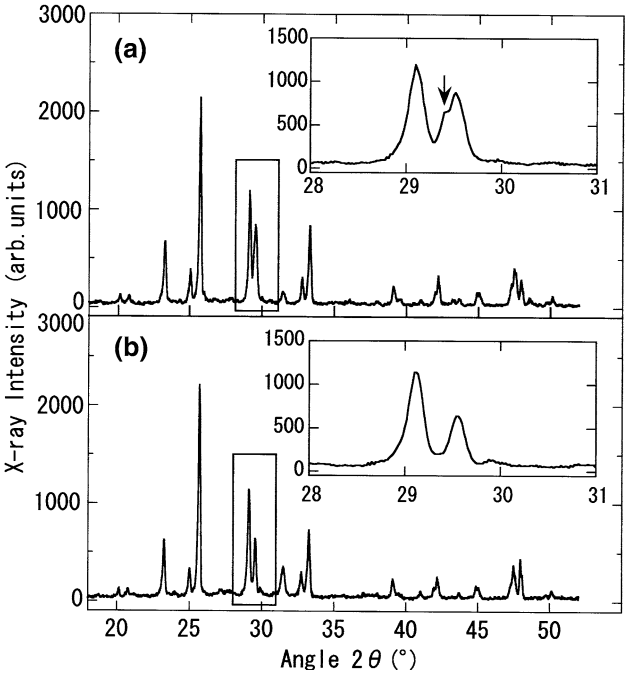

Fig. 4 X-ray patterns of **a** natural and **b** heat-treated scapolite #2 (1,000°C, 30 min). The diffraction line shown by an *arrow* in an *inset* in (**a**) corresponds to the strongest diffraction line due to calcite. The X-ray used was Cu$K\alpha_{1,2}$. The diffraction lines due to Cu$K\alpha_2$ were automatically deleted using a computer software

Table 1 shows the chemical compositions and the meionite ratios x of the four samples examined using the EPMA; natural #1, heat-treated #1 (1,000°C, 30 min), natural #2 and heat-treated #2 (1,000°C, 30 min). In calculating the chemical compositions, we normalized the formula of scapolite to $Si + Al = 12$. The meionite ratio x in scapolite was determined from the data in Table 1 using the following equation:

$$\begin{aligned}&\text{Scapolite } (\mathrm{Na,Ca})_4\mathrm{Al_3(Al,Si)_3Si_6O_{24}(Cl,CO_3)}\\&= \text{Marialite } (1-x)\mathrm{Na_4Al_3Si_9O_{24}Cl}\\&\quad + \text{Meionite } x\mathrm{Ca_4Al_6Si_6O_{24}CO_3}.\end{aligned} \quad (1)$$

The meionite ratios x of the four samples, natural #1, heat-treated #1 (1,000°C, 30 min), natural #2 and heat-treated #2 (1,000°C, 30 min), were determined to be 0.329, 0.332, 0.348 and 0.343, respectively. The differences of the meionite ratios x between natural and heat-treated samples were insignificant. The meionite ratios x of heat-treated scapolite #2 determined using the EPMA ranged from 0.318 to 0.391. This indicates that the composition of meionite is nonuniform in scapolite. The compositions of SO_3 in the four samples, natural #1, heat-treated #1 (1,000°C, 30 min), natural #2 and heat-treated #2 (1,000°C, 30 min), were 0.94, 0.91, 0.10 and 0.05 (wt%), respectively, (Table 1).

In the rough measurement using the ICP-OES, the presence of Ti, Fe, Mn, P, S, Sr, Ce and Eu was found in the four samples, natural #1, heat-treated #1 (1,000°C,

Table 1 Chemical compositions (wt%) and meionite ratio x of scapolites examined using EPMA; natural #1, heat-treated #1 (1,000°C, 30 min), natural #2 and heat-treated #2 (1,000°C, 30 min)

	Natural #1 $n^a = 10$	Heat-treated #1 $n^a = 10$	Natural #2 $n^a = 10$	Heat-treated #2 $n^a = 20$	Standard
SiO_2	54.76	54.28	54.08	55.45	Albite
Al_2O_3	23.12	23.00	23.31	23.79	Kyanite
TiO_2	0.02	0.02	0.02	0.01	$SrTiO_3$
FeO	0.01	0.02	0.02	0.02	Hematite
MnO	0.01	0.01	0.00	0.02	Rhodonite
MgO	0.00	0.00	0.00	0.00	Periclase
CaO	7.52	7.91	8.69	8.58	Wollastonite
Na_2O	9.59	9.20	8.67	7.69	Albite
K_2O	0.85	0.88	0.74	2.09	K-feldspar
Cl	2.28	2.27	2.44	1.51	Tugtupite
SO_3	0.94	0.91	0.10	0.05	Celestite
F	0.04	0.07	0.05	0.06	Fluorite
P_2O_5	0.01	0.01	0.01	0.18	Apatite
Ce_2O_3	0.04	0.05	0.04	0.03	CeF_3
Eu_2O_3	0.02	0.01	0.00	0.02	EuF_3
O = Cl	−0.51	−0.51	−0.55	−0.34	
O = F	−0.02	−0.03	−0.02	−0.03	
Total	98.68	98.10	97.60	99.13	
Meionite ratio x	0.329	0.332	0.348	0.343	

[a] Analyzed spots

30 min), natural #2 and heat-treated #2 (1,000°C, 30 min). Table 2 shows the contents of trace elements, S and Fe, in these samples, determined by detailed measurement using the ICP-OES. The contents of S and Fe were slightly different between natural and heat-treated samples, but the effect of heat treatment on the contents of S and Fe was unclear.

Figure 5a, b shows the PL spectra of natural scapolite #1 and heat-treated scapolite #1 (1,000°C, 30 min), respectively, at 300, 80 and 10 K, obtained under 390 nm excitation. As shown in Fig. 3, the relative PL intensity of heat-treated scapolite #1 was about 11 times as high as that of natural scapolite #1 at 300 K under the same measurement conditions. As the temperature decreased, the structure with a series of maxima spaced 15–30 nm became more distinct, and the PL spectrum at 10 K became a pectinate feature. After the heat treatment, narrow bands in the PL spectra at low temperatures became broad, and the dips between the narrow bands became shallow.

Table 2 Contents (mg/g) of trace elements in scapolites examined using ICP-OES; natural #1, heat-treated #1 (1,000°C, 30 min), natural #2 and heat-treated #2 (1,000°C, 30 min)

Element	Natural #1	Heat-treated #1	Natural #2	Heat-treated #2
S	2.48	3.08	0.97	0.95
Fe	1.03	1.12	1.25	0.86

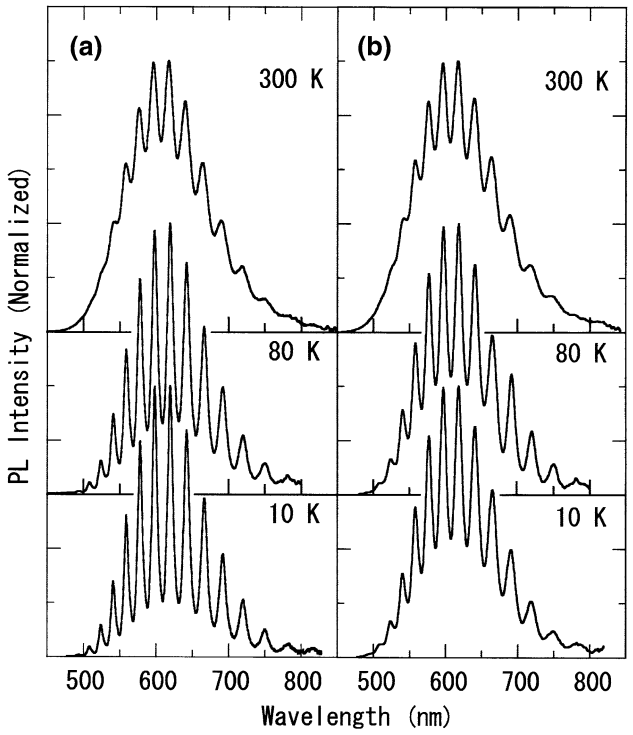

Fig. 5 PL spectra of scapolites, obtained at 300, 80 and 10 K under 390 nm excitation; **a** natural and **b** heat-treated scapolite #1 (1,000°C, 30 min)

Figure 6 (left) shows the excitation spectra of natural scapolite #1 at 300, 80 and 10 K, obtained by monitoring yellow luminescence at 596 nm. The excitation spectrum at 300 K consisted of the main band with a peak at 393 nm and a full width at half maximum (FWHM) of 57 nm. As the temperature decreased, the structure with a series of maxima spaced 5–9 nm became distinct on the main band. In addition to the main band, two small excitation bands at wavelengths 233 and 285 nm were observed. The slopes of the curves at wavelengths 200–220 nm indicate that there is another band at a wavelength shorter than 200 nm.

Although figures are not shown, the excitation spectra of the yellow luminescence from heat-treated scapolite #1 (1,000°C, 30 min) were also obtained at 300, 80 and 10 K. The main excitation band had a peak at 387 nm and a FWHM of 79 nm, and showed only an obscure structure even at 10 K.

Figure 7 shows the vibronic structures observed on the excitation (Ex) and emission (Em) bands of natural scapolite #1 at 10 K. Tables 3 and 4 show the peak wave numbers ν (kcm^{-1}) of narrow bands and the intervals (cm^{-1}) between the neighboring narrow bands of the emission and excitation spectra, respectively, in Fig. 7. The corresponding data obtained by Burgner et al. (1978) are also listed on the right-hand sides of Tables 3 and 4. The vibronic structure observed on the emission band started from

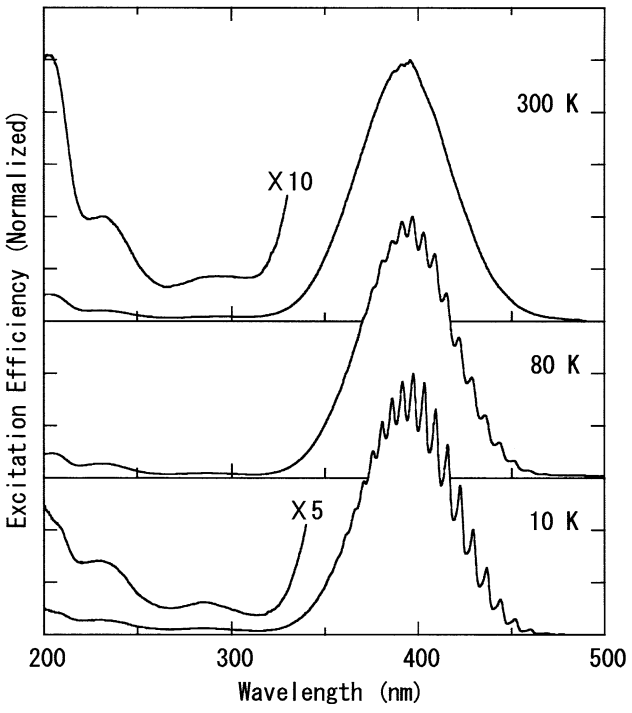

Fig. 6 Excitation spectra of natural scapolite #1 at 300, 80 and 10 K, obtained by monitoring yellow luminescence at 596 nm. Excitation spectra at short wavelengths at 300 and 10 K are magnified ×10 and ×5, respectively

the zero-phonon band at 20.881 kcm^{-1} (478.9 nm). The interval between the neighboring narrow bands decreased from 613 cm^{-1} for v'' = 1 to 540 cm^{-1} for v'' = 15. On the other hand, the vibronic structure observed on the excitation band started from the zero-phonon band at 20.921 kcm^{-1} (478.0 nm). The interval between the neighboring narrow bands decreased from 406 cm^{-1} for v' = 1 to 340 cm^{-1} for v' = 18.

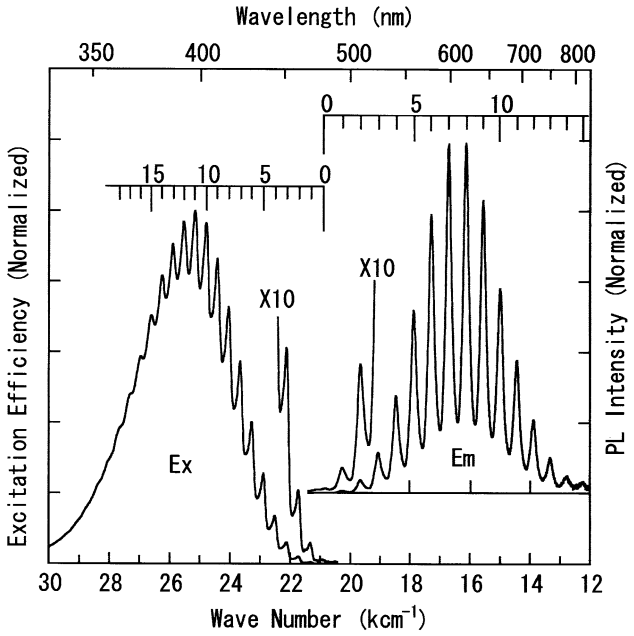

Fig. 7 Vibronic structures observed on the excitation (Ex) and emission (Em) bands of natural scapolite #1 at 10 K. Ex was obtained by monitoring yellow luminescence at 596 nm, and Em was obtained under 390 nm excitation. Excitation spectrum at long wavelengths and emission spectrum at short wavelengths are magnified ×10

Table 3 Peak wave numbers v (kcm^{-1}) of narrow emission bands due to S_2^- in scapolite shown in Fig. 7

v''	This work v (kcm^{-1})	Burgner et al. v (kcm^{-1})
0	20.881	20.752
1	20.268 (613)	20.145 (607)
2	19.666 (602)	19.542 (603)
3	19.069 (597)	18.946 (596)
4	18.477 (592)	18.354 (592)
5	17.892 (585)	17.766 (588)
6	17.310 (582)	17.185 (581)
7	16.731 (579)	16.607 (578)
8	16.155 (576)	16.031 (576)
9	15.584 (571)	15.462 (569)
10	15.017 (567)	14.896 (566)
11	14.457 (560)	14.334 (562)
12	13.902 (555)	
13	13.351 (551)	
14	12.804 (547)	
15	12.264 (540)	

Values in parentheses are intervals (cm^{-1}) from neighboring high-energy bands. The corresponding data obtained by Burgner et al. (1978) are listed on the right-hand side

The peak wave numbers v (cm^{-1}) of vibronic structures in the absorption and emission spectra of diatomic molecules are given by the following formula (Herzberg 1950):

$$v = v_{00} + \omega'_0 v' - \omega'_0 x'_0 v'^2 + \omega'_0 y'_0 v'^3 + \cdots - \left(\omega''_0 v'' - \omega''_0 x''_0 v''^2 + \omega''_0 y''_0 v''^3 + \cdots\right), \quad (2)$$

where v_{00} is the wave number difference between the vibrational level with the quantum number v' = 0 in the excited state and the vibrational level with the quantum number v'' = 0 in the ground state, ω_0' and ω_0'' are the fundamental vibrational energies of the excited and ground states, respectively, and $\omega_0'x_0'$, $\omega_0'y_0'$, $\omega_0''x_0''$ and $\omega_0''y_0''$ are anharmonicity parameters. The coefficients $\omega_0'y_0'$ and $\omega_0''y_0''$ are usually very small and can often be neglected. If we apply Eq. (2) to optical spectra at low temperatures, the peak wave numbers v_{em} (cm^{-1}) and v_{ex} (cm^{-1}) of vibronic structures in the emission and excitation spectra, respectively, are given by the following formulae:

Table 4 Peak wave numbers v (kcm^{-1}) of narrow excitation bands due to S_2^- in scapolite shown in Fig. 7

v'	This work v (kcm^{-1})	Burgner et al. v (kcm^{-1})
18	27.647 (340)	
17	27.307 (346)	
16	26.961 (351)	
15	26.610 (356)	
14	26.254 (361)	
13	25.893 (363)	25.907 (377?)
12	25.530 (366)	25.530 (338?)
11	25.164 (369)	25.192 (378)
10	24.795 (375)	24.814 (382)
9	24.420 (376)	24.432 (385)
8	24.044 (381)	24.047 (378)
7	23.663 (380)	23.669 (775?)
6	23.283 (384)	Lack
5	22.899 (387)	22.894 (387)
4	22.512 (393)	22.507 (395)
3	22.119 (394)	22.112 (396)
2	21.725 (398)	21.716 (796?)
1	21.327 (406)	Lack
0	20.921	20.920

Values in parentheses are intervals (cm^{-1}) from neighboring low-energy bands. The corresponding data obtained by Burgner et al. (1978) are listed on the right-hand side

$$\nu_{em} = \nu_{00} - \omega''_0 v'' + \omega''_0 x''_0 v''^2 \quad (3)$$

and

$$\nu_{ex} = \nu_{00} + \omega'_0 v' + \omega'_0 x'_0 v'^2. \quad (4)$$

The spectroscopic constants obtained by fitting Eqs. (3) and (4) to the experimental data in Tables 3 and 4 are listed in Table 5, where the spectroscopic constants of S_2^- in scapolite (Burgner et al. 1978) and KI (Rebane and Rebane 1974) are also listed.

Table 5 Spectroscopic constants for ground and excited states of S_2^- in scapolite and KI

State	ν_{00} (kcm^{-1})	ω_0 (cm^{-1})	$\omega_0 x_0$ (cm^{-1})
Ground State			
S_2^- in scapolite	20.881	611	2.6
S_2^- in scapolite[a]	20.808	607	2.1
S_2^- in KI[b]	20.026	598.6	2.2
Excited State			
S_2^- in scapolite	20.921	405	1.8
S_2^- in scapolite[c]	20.920	399	1.0

[a] Under 454.5 nm excitation (Burgner et al. 1978)

[b] Rebane and Rebane 1974

[c] Burgner et al. 1978

Discussion

As shown in Table 1, the meionite ratios x in natural scapolites #1 and #2 were 0.329 and 0.348, respectively. In accordance with the nomenclature of Shaw (1960), our samples were identified to be dipyre, Me_{20}–Me_{50}. In calculating the chemical compositions, we normalized the formula of scapolite to $Si + Al = 12$. A divalent Fe^{2+} ion substitutes for Na^+ or Ca^{2+} in scapolite, and a trivalent Fe^{3+} ion substitutes for Si^{4+} or Al^{3+}. If the chemical content of Fe in our samples is large, we should renormalize the formula to $Si + Al + Fe^{3+} = 12$. It was reported by Shaw (1960) that some natural scapolites contain 1.5–2.0 wt% Fe_2O_3. However, the chemical composition of FeO in our samples was only 0.02 wt% (Table 1), and the content of Fe in our samples examined using the ICP-OES was only about 1 mg/g (Table 2).

As shown in Fig. 2, the relative efficiency of yellow luminescence from scapolite #2 was increased up to 117 times by heat treatment at 1,000°C for 2 h in air. The effect of heat treatment did not depend on the sample form, powder or broken piece. This indicates that the increase in the efficiency of S_2^- luminescence caused by heat treatment is not affected by the oxidation atmosphere.

In sodalite containing sulfur, we can observe orange–yellow fluorescence due to S_2^- in the cubo-octahedral cages consisting of AlO_4 and SiO_4 tetrahedra (Aierken et al. 2007). McLaughlan and Marshall (1970) suggested the presence of S_3^- clusters in synthetic sulfur-doped sodalite on the basis of the results from the EPR measurement. The above results also suggest that scapolite includes S_3^- clusters. In lead-activated alkali halides, Pb clusters are resolved into isolated Pb^{2+} centers by heating samples to 400–700°C for 10–60 min and successive quenching. An activator is mobile in a crystal at room temperature and aggregates to form Pb clusters in 2–5 h after thermal quenching (Dryden and Harvey 1969; Collins and Crawford Jr 1972). However, the efficiency of yellow luminescence from scapolite did not depend on the speed of thermal quenching and was stable in 6 months after thermal quenching. This suggests that the increase in the efficiency of S_2^- luminescence caused by heat treatment is not affected by the decomposition of sulfur clusters, such as S_3^- clusters to S_2^- centers in scapolite.

The relative efficiency of yellow luminescence from scapolite #2 was increased up to about 85 times by heat treatment at 1,000°C for 30 min in air (Figs. 2, 3). It was ascertained by X-ray diffraction analysis that the crystal structure of scapolite #2 is unchanged by heat treatment, except that a minor inclusion of calcite in the untreated sample was decomposed by heat treatment in air (Fig. 4a, b). The contents of sulfur as a trace element in natural and heat-treated scapolites #2 analyzed using the ICP-OES were 0.97 and 0.95 mg/g, respectively, and were almost unchanged by heat treatment (Table 2).

The dominant S species in scapolite are SO_3^{2-} and SO_4^{2-} (Chappell and White 1968; Swayze and Clark 1990; Teertstra and Sherriff 1996). From the facts described above, we may conclude that the increase in the efficiency of S_2^- luminescence caused by heat treatment is ascribed to the alteration of SO_3^{2-} and SO_4^{2-} to S_2^- in scapolite.

As shown in Fig. 2, the relative efficiency of yellow luminescence from scapolite #2 was decreased by heat treatment at temperatures below 800°C. Regrettably, the present authors cannot give a reason for the decrease in the luminescence efficiency.

As mentioned above, the emission and excitation spectra of the S_2^- center in scapolite have been reported by some investigators (Kirk 1955; Tarashchan 1978; Burgner et al. 1978; Curie et al. 1981; Prokofiev et al. 1982). The peak wavelengths of the S_2^- emission bands, however, do not agree. We presume that our spectra in Figs. 3, 5, 6 and 7 show the reliable curves of the emission and excitation spectra of S_2^- in scapolite at 300, 80 and 10 K, because we carefully corrected the measured spectra as described in the experimental section.

Burgner et al. (1978) observed vibronic structures on the emission and excitation bands of S_2^- centers in scapolite at 4.2 K. Emission spectra were observed under 454.5–

476.5 nm excitation using an Ar^+ laser and were not corrected for photomultiplier response. These excitation wavelengths correspond to the lowest-energy end of the excitation band, where the excitation efficiency is very low. They indicated that yellow luminescence is enhanced by heating samples to 900°C for 24 h. The effect of heat treatment on the luminescence was not described. The excitation band of the S_2^- luminescence of heat-treated scapolite at 4.2 K consisted of a band located at about 400 nm and showed a series of more than 14 vibronic bands on the low-energy half (Burgner et al. 1978). On the right-hand side of Table 4, we listed the peak wave numbers written in Table 1 and Fig. 4 of the paper by Burgner et al. (1978). We note that Fig. 4 of the paper by Burgner et al. (1978) is incorrect. In Fig. 4 of the paper by Burgner et al. (1978), 11 wave numbers were written on a series of maxima. The energy interval 775 cm^{-1} between 22.894 and 23.669 kcm^{-1} is about twice as large as the energy intervals 380–390 cm^{-1} between other wave numbers. This indicates that there is a lack between the two wave numbers. Therefore, the wave numbers of 23.669 (kcm^{-1}) and larger correspond to the neighboring peaks at short wavelengths. Moreover, the excitation curve was drawn at long wavelengths by about 4 nm compared with the correct curve.

In our previous paper (Aierken et al. 2007), we reported the details of the narrow bands of S_2^- luminescence from heat-treated sodalite at 10 K. Each narrow band showed a fine structure consisting of a small peak due to the stretching vibration of the isotopic species of $^{32}S^{34}S^-$, a main peak due to that of the isotopic species of $^{32}S_2^-$ and five peaks due to the phonon sidebands of the main peak. The pectinate structure with a series of maxima in natural scapolite #1 at 10 K is more pronounced than that in heat-treated sodalite at 10 K, but no fine structure is observed on the narrow bands of S_2^- luminescence from natural scapolite #1 [Figs. 5a, 7 (right)]. The relative efficiency of yellow luminescence from scapolite is markedly increased by heat treatment. However, the dips between the narrow bands of heat-treated scapolite #1 at 10 K become shallow after heat treatment (Fig. 5), and no fine structure is observed on the narrow bands of S_2^- luminescence from heat-treated scapolite #1 (Fig. 5b). In another expression, the feature of the PL spectrum of S_2^- in heat-treated scapolite #1 at 10 K corresponds to that in natural scapolite #1 at temperature higher than 80 K (Fig. 5). These phenomena are explained by the fact that S_2^- in scapolite is placed in various aluminosilicate environments, because scapolite is a solid solution of marialite and meionite. As mentioned above, the meionite ratios x of heat-treated scapolite #2 determined using the EPMA ranged from 0.318 to 0.391. The electronic transitions in the S_2^- centers in scapolite are affected by crystal vibrations with various modes, and the spectral shapes are diffused. In contrast to scapolite, the narrow emission band of S_2^- in KI at 10 K consists of sharp lines (Rebane and Rebane 1974), because S_2^- in KI is placed in a simple crystal environment.

As shown in Fig. 6, the excitation spectra consist of a main band at 393 nm, two small bands at 233, 285, and a third small band at a wave length shorter than 200 nm. The main band is clearly ascribed to the reverse transition of yellow luminescence due to S_2^- in scapolite. The origin of the small excitation band at a wavelength shorter than 200 nm may be ascribed to the fundamental absorption of scapolite. The other two small excitation bands at 233 and 285 nm may be ascribed to minor impurities in the sample, the origin that is unknown. The main excitation band shows a distinct vibronic structure at 10 K. Similar vibronic structures are observed on the excitation bands of S_2^- in heat-treated scapolite at 4.2 K (Burgner et al. 1978) and sulfur-added KI at 4.2 K (Rebane and Rebane 1974).

Figure 7 and Tables 3 and 4 show the vibronic structures observed on the excitation and emission bands of S_2^- in natural scapolite #1 at 10 K. There is a small difference between the peak energies of the zero-phonon bands of the excitation and emission bands, which are 20.921 kcm^{-1} (478.0 nm) and 20.881 kcm^{-1} (478.9 nm), respectively. This may be caused by the fact that the zero-phonon bands consist of several zero-phonon lines, which correspond to the energy levels of S_2^- centers with different aluminosilicate environments, because scapolite is a solid solution of marialite and meionite. Burgner et al. (1978) observed six zero-phonon lines at 20.677, 20.752, 20.808, 20.986, 21.024 and 21.057 kcm^{-1} in the emission spectrum of S_2^- in scapolite under laser excitation. As shown in Table 4, the peak energies of our zero-phonon band (20.921 kcm^{-1}) and the zero-phonon line (20.920 kcm^{-1}) observed by Burgner et al. (1978) in the excitation band of scapolite are in good agreement.

Concluding remarks

The PL and excitation spectra of S_2^- in scapolite at 300, 80 and 10 K were presented. The pronounced structures due to the symmetric vibration of sulfur atoms in S_2^- centers were observed on both the emission and excitation bands. It was found that the relative luminescence efficiency of yellow luminescence is markedly increased by heat treatment in air. The enhancement of yellow luminescence by heat treatment is ascribed to the alteration of SO_3^{2-} and SO_4^{2-} to S_2^- in scapolite.

Acknowledgments The chemical compositions of natural and heat-treated scapolites were determined using the EPMA at the Research Instruments Center, Okayama University of Science. The analysis of the contents of trace elements in scapolite was carried out using the

ICP-OES at the Xinjiang Technical Institute of Physics and Chemistry, the Chinese Academy of Sciences. The authors are also grateful to Mr. Zhi-Hui Chen for performing the ICP-OES analysis. This study was supported by the National Natural Science Foundation of China (Grant No. 10764004) and funded by the Scientific Research Program of the Higher Education Institution of Xinjiang, China (Grant No. XJEDU2006149).

References

Aierken Sidike, Alifu Sawuti, Wang X-M, Zhu H-J, Kobayashi S, Kusachi I, Yamashita N (2007) Fine structure in photoluminescence spectrum of S_2^- center in sodalite. Phys Chem Miner 34:477–484

Burgner RP, Scheetz BE, White WB (1978) Vibrational structure of the S_2^- luminescence in scapolite. Phys Chem Miner 2:317–324

Chappell BW, White JR (1968) The X-ray spectrographic determination of sulfur coordination in scapolite. Am Mineral 53:1735–1738

Collins WC, Crawford JH Jr (1972) Polarization of luminescence in NaCl:Pb^{2+} and KCl:Pb^{2+}. Phys Rev B 5:633–641

Curie D, Canny B, Jaszczyn-Kopec P, Liu HK, Berry D, Williams F (1981) The effects of hydrostatic and uniaxial pressures on vibronic spectra. J Lumin 24/25:145–154

Dryden JS, Harvey GG (1969) Dielectric and optical properties of lead-activated sodium and potassium chloride crystals. J Phys: Solid State Phys 2:603–618

Gorobets BS, Rogojine AA (2002) Luminescence spectra of minerals. Reference Book. (translated from Russian by Gorobets B and Girnis A) RPC VIMS, Moscow pp 148–149, 262

Herzberg G (1950) Molecular spectra and molecular structure, vol 1 Spectra of Diatomic Molecules, 2nd ed., D. van Nostrand Company, Inc., Princeton p 151

Ikezawa M, Rolfe J (1973) Zero-phonon transitions in O_2^-, S_2^-, Se_2^-, and SeS^- molecules dissolved in alkali halide crystals. J Chem Phys 58:2024–2038

Kirk RD (1955) The luminescence and tenebrescence of natural and synthetic sodalite. Am Mineral 40:22–31

Kirk RD, Schulman JH, Rosenstock HB (1965) Structure in the luminescence emission of the S_2^- ion. Solid State Comm 3:235–239

Lin SB, Burley BJ (1975) The crystal structure of an intermediate scapolite-wernerite. Act Crystallogr B 31:1806–1814

Marfunin AS (1979) Spectroscopy, luminescence and radiation centers in minerals. (translated from Russian by Schiffer VV) Springer, Berlin, pp 216–217, 279–283

McLaughlan SD, Marshall DJ (1970) Paramagnetic resonance of sulfur radicals in synthetic sodalites. J Phys Chem 74:1359–1363

Prokofiev IV, Gorobets BS, Gaft ML, Lurie YuS (1982) Rare-earth centers of luminescence in leucophanite, shortite, meionite and monazite. Mineralogical Papers, Lvov State University, Vyshcha Shkola 36:76–79 (in Russian), through Gorobets and Rogojine (2002)

Rebane KK, Rebane LA (1974) Small molecular ions as impurity centers in crystals. Pure Appl Chem 37:161–181

Rolfe J (1964) Low-temperature emission spectra of O_2^- in alkali halides. J Chem Phys 40:1664–1670

Rolfe J (1968) Emission spectra of S_2^-, Se_2^-, and SeS^- ions in KI crystals. J Chem Phys 49:4193–4197

Rolfe J, Lipsett FR, King WJ (1961) Optical absorption and fluorescence of oxygen in alkali halide crystals. Phys Rev 123:447–454

Seto Y, Shimobayashi N, Miyake A, Kitamura M (2004) Composition and $I4/m$-$P4_2/n$ phase transition in scapolite solid solutions. Am Mineral 89:257–265

Shaw DM (1960) The geochemistry of scapolite. Part I. Previous work and general mineralogy. J Petrol 1:218–260, Part II. Trace elements, petrology, and general geochemistry. J Petrol 1:261–285

Swayze GA, Clark RN (1990) Infrared spectra and crystal chemistry of scapolites: Implications for Martian mineralogy. J Geophys Res 95:14481–14495

Tarashchan AN (1978) Luminescence of minerals. Kiev: Naukova Dumka (in Russian), through Marfunin (1979); Gorobets and Rogojine (2002)

Teertstra DK, Sherriff BL (1996) Scapolite cell-parameter trends along the solid-solution series. Am Mineral 81:169–180